International Journal of Paleopathology 52 (2026) 11–19

Contents lists available at ScienceDirect

International Journal of Paleopathology

journal homepage: www.elsevier.com/locate/ijpp

Case study

A possible case of hypertrophic osteopathy in osteological remains representing cattle hide processing from a Roman villa in England

Fay Worley [a,1,*], G. Michael Taylor [b,2], Orestis L. Katsamenis [c,d,3], Simon Mays [a,e,f,4]

[a] Historic England, Fort Cumberland, Portsmouth PO4 9LD, United Kingdom
[b] School of Biosciences and Medicine, University of Surrey, AX Building, Stag Hill Campus, Guildford GU2 7XH, United Kingdom
[c] μ-VIS X-ray Imaging Centre, Faculty of Engineering and Physical Sciences, University of Southampton, Southampton SO17 1BJ, United Kingdom
[d] Institute for Life Sciences, University of Southampton, University Road, Highfield, Southampton SO17 1BJ, United Kingdom
[e] School of History, Classics and Archaeology, University of Edinburgh, United Kingdom
[f] Department of Archaeology, University of Southampton, United Kingdom

ARTICLE INFO

Keywords:
Periosteal new bone
Vascular foramen
Faunal remains
X-ray microfocus Computed Tomography (μCT)

ABSTRACT

Objective: To evaluate the likelihood that pathological features noted on cattle bones indicate that the animal suffered hypertrophic osteopathy.
Materials: Cattle bones, mostly from the lower extremities, representing a single individual, recovered from a Romano-British villa (4th century CE).
Methods: The remains were subject to macroscopic, low-power microscopic, radiographic and μCT study, as well as biomolecular analysis for *M. tuberculosis* complex and *Brucella* species DNA.
Results: The remains represent a single individual and show bilaterally symmetrical subperiosteal new bone formation with no micro-anatomical alteration of the underlying bone structure. aDNA analysis was negative for *M. tuberculosis* and *Brucella,* but positive for bovine mitochondrial DNA (mtDNA).
Conclusions: Hypertrophic osteopathy is the most likely differential diagnoses.
Significance: Hypertrophic osteopathy is uncommon in bovids, and this is the first suspected case in livestock remains from an archaeological site. It demonstrates the importance of differential diagnosis in disarticulated remains through recognition of skeletal patterning.
Limitations: The diagnosis is hampered by the incomplete nature of the remains.
Suggestions for further research: Given the primacy of chronic infection as a cause of hypertrophic osteopathy in the past, scanning these remains for evidence of pathogens using Next Generation Sequencing when feasible, and other biomolecular techniques may be useful.

1. Introduction

Hypertrophic osteopathy (HO) is a condition wherein the prime skeletal manifestation is diffuse subperiosteal new bone (PNB) deposition in a distinct bilaterally symmetrical pattern, particularly in appendicular elements (Mays and Taylor, 2002; Huang et al., 2010; Lewis et al., 2011). It generally arises as a secondary condition in response to intra-thoracic (or more rarely intra-abdominal) disease, via mechanisms that remain incompletely understood (Cetinkaya et al., 2011). It is often associated with neoplastic or chronic infectious disease, such as tuberculosis (see discussion in Mays and Taylor, 2002), and affects humans (Resnick and Niwayama, 1995: 4427–4434), and a wide variety of other species (Craig et al., 2015: 93).

In the veterinary literature, HO has been most thoroughly described in the dog (Brodey, 1971; Withers et al., 2013), but amongst domestic species, its occurrence has also been confirmed in horses (Enright et al.,

* Corresponding author.
E-mail addresses: Fay.Worley@HistoricEngland.org.uk (F. Worley), Gm.taylor@surrey.ac.uk (G.M. Taylor), Simon.Mays@HistoricEngland.org.uk (S. Mays).
[1] ORCID: 0000–0003-3618–4027.
[2] ORCID: 0000–0002-4215–3916.
[3] ORCID: 0000–0003-4367–4147.
[4] ORCID:0000–0002-0352–5625.

https://doi.org/10.1016/j.ijpp.2025.11.003
Received 12 November 2024; Received in revised form 3 November 2025; Accepted 9 November 2025
Available online 28 November 2025

Fig. 1. Location of Groundwell Roman Villa.

2011), cats (Becker et al. 1999), sheep (Bom et al., 2020), goats (Heacock et al., 2020) and cattle (Guyot et al., 2011). Veterinary cases in cattle describe skeletal involvement as PNB formation on the appendicular skeleton (László, 1929; Hofmeyr, 1964; Martin et al., 1971; Merritt et al., 1971; Schelcher et al., 1989; Ravary and Fecteau, 2000; Guyot et al., 2011), always implicating metapodials, and usually extending proximally as far as the radius, ulna or tibia, exceptionally to the entire appendicular skeleton (László 1929). Phalangeal involvement is seen in almost all cases but not described in detail.

While case reports describing HO in human remains from archaeological sites have accumulated in palaeopathology publications (Loyer et al., 2019: 67, table 1), adequate identifications of HO in faunal palaeopathology are few, doubtless reflecting the special difficulties that attend identification of the condition in archaeofaunal remains, alongside its low modern prevalence in many of these species.

Of prime importance in distinguishing HO from other potential causes of PNB formation is the distinct bilateral symmetry in PNB deposits seen in HO, a pattern that appears to apply across species (Resnick and Niwayama, 1981: 2983–2996; Allan, 2007: 351, Marinkovich et al., 2019). The faunal record characteristically comprises commingled, disarticulated bone fragments representing food, butchery, industrial or other waste. This normally precludes assessment of the overall distribution of lesions in individual animals, leaving one reliant upon lesion morphology and perhaps intra-element distribution if the affected bone is sufficiently complete.

In general, morphology of PNB deposits is of limited value when inferring their aetiology, depending more upon factors such as the duration of osteological involvement in disease and whether lesions were active at time of death (Weston, 2008). The radiographic and dry-bone histologic appearance of deposits are likewise rather aetiologically non-specific (Weston, 2009). Patterning of deposits within skeletal elements may augment differential diagnosis (see below) but can be highly variable in HO and inconsistent between species (e.g., Gall et al. 1951; Johnson and Watson, 2000). In practice, it is of limited diagnostic value. Thus, although some palaeopathologists have attempted to suggest the presence of HO using isolated elements showing PNB deposits (e.g., Luff and Brothwell, 1993: 117), the inability

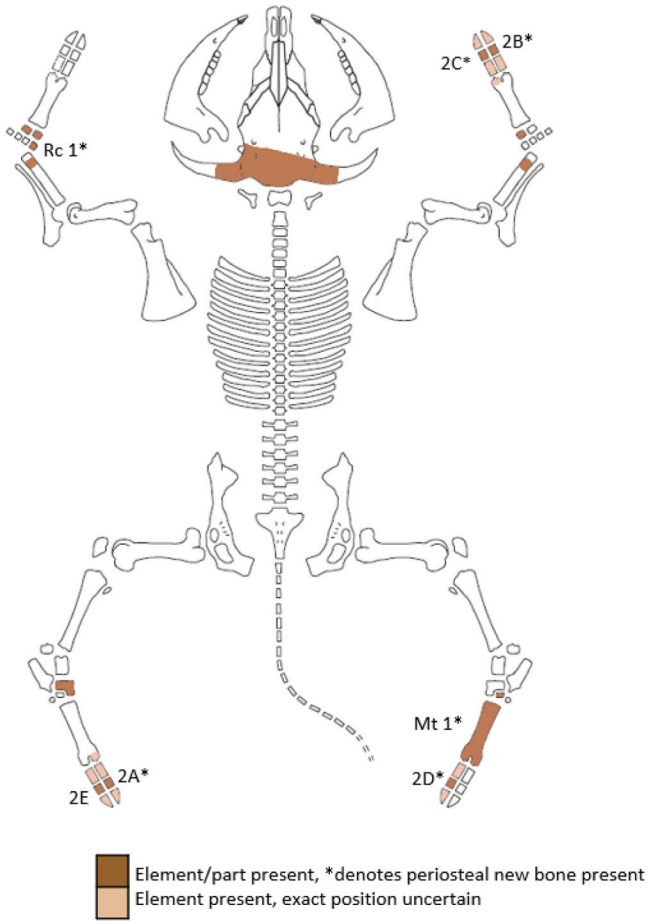

Fig. 2. Skeletal representation of cattle bones. Second phalanges (2A–2E), metatarsal (Mt 1) and radial carpal (Rc 1) labelled. Skeleton diagram adapted from M Coutureau (Inrap) © 2013, reviewed by Bemilli, C (Inrap), December 2022, ArcheoZoo.org. Licence: Attribution-NonCommercial-ShareAlike 4.0 International CC BY-NC-SA 4.0 Deed; after Helmer (1987)

Table 1
Skeletal position of phalanges.

First phalanges		Second phalanges		Third phalanges	
ID	**Position**	**ID**	**Position**	**ID**	**Position**
1A	Hind, LIII or RIV	2A*	Hind, LIII	3A	Hind
1B	Fore, LIII or RIV	2B*	Fore, RIV?	3B	Fore?
1C	Fore, LIV or RIII	2C**	Fore, RIII?	3C	Fore?
1D	Hind? LIV or RIII	2D**	Hind, RIII	3D	Indeterminate
1E	Hind, LIV or RIII	2E	Hind, LIV	3E	Hind

* small lesion; **large lesion. Position: L left; R right; Roman numerals denote digit

to assess patterns of skeletal involvement has led to debate over diagnosis in specific specimens (see, for example, Baker and Brothwell, 1980: 162 vs Drexler, 1957 regarding an isolated cave bear humerus).

We are aware of only two secure examples of HO reported in faunal material from archaeological sites; both from North America, and both canid remains that can be ascribed to single individuals on the basis of the archaeological context. Bathurst and Barta (2004) report HO in a fully articulated dog burial from 16th century Ontario, Canada and Lawler et al. (2015) report a case from a domestic dog from Iowa, USA, dated 7430–7020 cal BP. The Iowa case was not an articulated burial, but elements were ascribed to a single animal based on contextual association and size similarities. Here, we present a differential diagnosis for what appears to be the first case of HO in archaeological cattle. We

Table 2
Subperiosteal lesions on cattle phalanges (all recovered bones listed).

Phalanx	Completeness	Fusion	Periostosis
First phalanges			
1A	C	U	-
1B	PEM	U	-
1C	PEO	U	-
1D	PEM	U	-
1E	C	U	-
Second phalanges			
2A	C	FO	Possible periostosis surrounding axial foramen, as evidenced by slight colour change, which may indicate the former presence of a lesion lost post-mortem.
2B	C	FO	Focussed periostosis surrounding axial foramen (5 mm diameter, defined edges).
2C	C	FO	Focussed periostosis (6 mm diameter, rising 1.5 m from surface, defined edges) surrounding axial foramen.
2D	C	FO	Focussed periostosis surrounding axial foramen (9 mm maximum diameter), the majority of which has been lost post-mortem. Its former extent is now visible as a granular surface texture with associated colour change.
2E	C	FO	-
Third phalanges			
3A	C	n/a	-
3B	C	n/a	-
3C	C	n/a	-
3D	P	n/a	-
3E	C	n/a	-

Completeness: C complete; P partial; PEM proximal epiphysis missing; PEO proximal epiphysis only
Fusion: FO fusion line open; U unfused

Table 3
Subperiosteal lesions on cattle limb bones, excluding phalanges (all recovered bones from individual listed).

Element	Side	Completeness	Fusion	Periostosis
Forelimb				
Radius	L	DDO	U	-
Radius	R	DDO	U	-
Radial carpal (Rc1)	L	C	n/a	Diffuse periostosis on medial aspect
Carpal III	L	C	n/a	-
Carpal III	R	C	n/a	-
Carpal IV	L	C	n/a	-
Hind limb				
Metatarsal (Mt1)	R	C (condyles refitted)	U	Diffuse periostosis on proximal dorsal and medial diaphysis.
Centroquartal	L	P	n/a	
Tarsal II + III	R	C	n/a	
Indeterminate limb				
Two metapodials (not a pair)	I	DEO	U	-

Side: L left; R right; I indeterminate.
Completeness: C complete (may have slight damage); DDO distal diaphysis only; DEO distal epiphysis only; P partial
Fusion: U unfused

use biological characteristics and context of deposition to interpret this pathology on an incomplete and disarticulated skeleton, in this case likely carcass processing waste.

2. Materials

The analysis focusses on 36 pieces of cattle (*Bos taurus*) bone hand collected from a demolition layer at Groundwell Roman Villa, Wiltshire, England (Fig. 1). The excavation report (Morley and Wilson, 2024) is in the final stages of production, with a summary of relevant areas of the villa structure in Morley and Wilson (2025). Radiocarbon determination of one of the elements (phalanx 1B) provides a date of cal A.D. 325–370 (95 % probability; SUERC-18221; see Meadows et al. 2012), confirming that the deposit is from the late Roman period.

3. Methods

The cattle remains had been washed prior to analysis. They were initially examined macroscopically and through low power microscopy. Age at death was estimated from epiphyseal union (Silver, 1969). The skeletal position of phalanges was determined following criteria from Bartosiewicz (1993), Dottrens (1946), Peters (1988) and comparison with nine specimens in the Historic England Zooarchaeological Reference Collection (see Supplementary Information).

Imaging was used to establish whether bones exhibited internal abnormalities. All intact remains were radiographed. X-radiography was undertaken at Fort Cumberland Laboratories, Portsmouth, using an AGO HS 225 kV Hi-Stability X-ray system. Analogue Kodak AA400 film was used to capture the images, exposed for 12 s at 1.2 m field focus distance using 3 mA and 70 kV (phalanges) or 80 kV (metatarsal).

The phalanx showing the most marked macroscopic alteration (phalanx 2C) was additionally selected for X-ray microfocus Computed Tomography (μCT) examination. μCT imaging was conducted to evaluate the volumetric manifestation of these alterations. μCT imaging was performed using a Nikon XTEK XTH 225 kVp micro-focus CT system at the μ-VIS X-ray Imaging Centre at the University of Southampton (https://muvis.org). Imaging was conducted at 150 kVp / 76 μA without any beam pre-filtration, with a voxel-edge size of 21.5 μm (cf. Supplementary Information for more details). Volumetric analysis and visualisation were conducted in "Dragonfly" (v. 2022.1; Object Research Systems (ORS) Inc, Montreal, Canada, 2020; software available at http://www.theobjects.com/dragonfly).

To inform differential diagnoses and to investigate the potential presence of tuberculosis or brucellosis, we conducted ancient DNA (aDNA) analysis for *Mycobacterium tuberculosis* (MTB) complex and for *Brucella* species DNA on phalanx 2A. Full details of the imaging and biomolecular methods are provided in Supplementary Information.

4. Results

4.1. Skeletal representation and age at death

All identified elements were from the cranium (fragments from both horncores and frontals) and all four distal limbs. There is no duplication of skeletal elements and epiphyseal closure suggests an age-at-death of approximately eighteen months, consistent with the porous texture of the horncores (Armitage, 1982). Sex could not be determined; both male and female cattle were horned in Roman Britain (Allen, 2017, 99, 104–5). Details of the elements present, and of the state of epiphyseal union, are presented in Fig. 2 and Tables 1–3.

4.2. Refitting bones and butchery marks

The closely refitting unfused phalangeal and metatarsal epiphyses indicate that the deposit had not been significantly disturbed after deposition. This is also indicated by closely refitting articulating elements, whose association is sometimes confirmed by bridging or aligned butchery marks (cranial fragments, the right metatarsal and tarsal II+III, *see below*), or arthropathy (opposing articular depressions and slight porosity and erosion on the proximal metatarsal and opposing face of the right tarsal II+III). These alterations are unrelated to the PNB and are not discussed further.

The butchery marks are clustered on the cranium and at the most proximal surviving parts of each limb. Those on the limbs can be interpreted as evidence of skinning or disarticulation of all feet: a cluster

Fig. 3. Carcass processing evidence. A) aligned transverse chop marks at anterior margin on both frontals (arrows); B) radii with symmetrical post-mortem fractures, seen at top of image; C) fine transverse cuts on dorsal and medial proximal metatarsal shaft (bottom arrow, see also Fig. 5), with cuts also bridging metatarsal and tarsal (top arrow).

of horizontal cuts on the right proximal metatarsal passing also onto the adjoining tarsal II+III (Fig. 3), a transverse chop through the left centroquartal, cuts on right carpal III and left radial carpal. The radii were broken transversely across the distal diaphysis in a symmetrical manner (Fig. 3), suggesting that the forelimbs were divided at this point. The skull was chopped transversely through the frontals and inferior to the horncores, leaving them attached to a connecting section of frontal bone (Fig. 3).

We assessed these remains as belonging to a single individual based on several lines of evidence:

- Non-duplication of elements.
- Consistent age-at-death estimates from several ageable elements.
- Closely refitting articular surfaces on different elements.
- Butchery marks bridging refitting and associated bones and fragments.
- Consistent expression of pathology on different elements.

4.3. Subperiosteal new bone proliferation

Four of the five second phalanges exhibited small circular deposits of PNB surrounding a foramen on their axial diaphyses (Fig. 4, Table 2), the similarity of location of lesions on the phalanges is striking. Pathological phalanges represent both hind feet and the right forefoot, with equivalent elements of the left forefoot not recovered. However, small deposits of more diffuse subperiosteal woven bone were also recorded on the left radial carpal (Table 3), meaning that all four feet are involved in the disease process. The complete metatarsal exhibited woven bone on the proximal two thirds of the dorsal and medial diaphysis (Fig. 5).

4.4. Radiographic (planar) and CT (volumetric) examination

Radiography revealed no evidence for pathological alterations to the internal structure of any appendicular elements. Phalanx 2C showed the most marked subperiosteal involvement, so might be expected to be the most likely to display internal alterations, should the disease process present potentially lead to such changes. It was therefore selected for CT examination. This indicated no endosteal abnormalities. The PNB around the vascular foramen was confined to the external cortex, was absent from the rim of the foramen and the lumen of the vascular channel (Fig. 6, 7 and 8 and Supplementary Information); Full dataset available at https://doi.org/10.5281/zenodo.8262662.

Supplementary material related to this article can be found online at doi:10.1016/j.ijpp.2025.11.003.

4.5. Biomolecular analysis

No evidence was found for any *Mycobacterium tuberculosis* (MTB) complex organisms in the extract prepared from phalanx 2A, despite repeated testing. Additionally, screening for *Brucella* genomic DNA was also negative. In contrast, we obtained evidence for survival of bovine mtDNA in the specimen, demonstrating that conditions favoured aDNA survival and also that PCR inhibitors were not responsible for the negative pathogen results. For further details see Supplementary Information (text and Supplementary Figures 1 and 2).

5. Differential diagnosis

The phalanges and the metatarsal exhibit PNB, the deposit on the metatarsal being diffuse, while those on the phalanges each focus on a

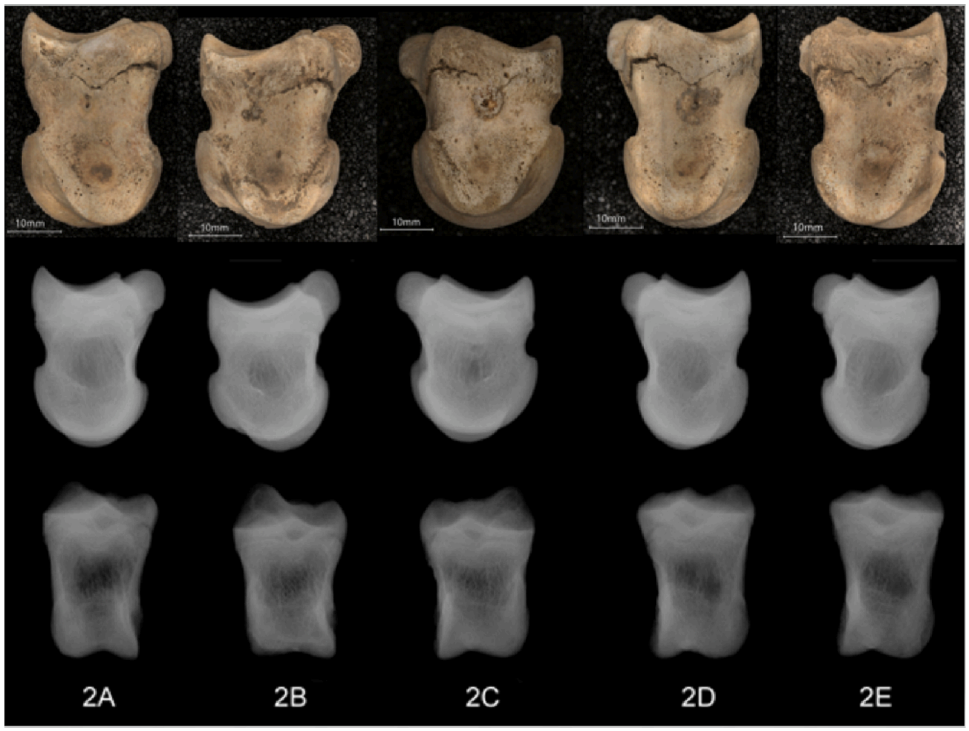

Fig. 4. Cattle second phalanges. Axial side photographed using AHRC funded Keyence VHX7000 3-D digital microscope at x20 magnification (AHRC Award AH/V011758/1) (top), x-radiographs showing mediolateral view (middle, x-ray P3324) and anterior-posterior view (bottom, x-ray P3322). Subperiosteal new bone (PNB) can be seen encircling the vascular foramina on several specimens with larger diameter lesions on 2C and 2D and smaller lesions on 2A and 2B; those of 2A and 2D being evidenced by remnant PNB and discolouration demarking former extent. Phalanx 2E does not exhibit a lesion. © Historic England.

specific locus; the vascular foramen on their axial aspects. All deposits are of unremodelled woven bone indicating that the condition was active at time of death, and the phalanges appear to have been involved approximately simultaneously rather than disease gradually spreading to different digits. The involvement of various skeletal regions (phalanges from at least three feet) and the similarity of the new bone deposits on them suggests a response to an active systemic condition rather than localised injury or disease of the extremities such as laminitis.

A wide variety of conditions may lead to systemic PNB formation. Our principle differential diagnoses are osteofluorosis, copper deficiency, panosteitis, systemic infection and hypertrophic osteopathy.

Osteofluorosis is a bony reaction to excess fluorine in the diet. Fluorine can be obtained directly from groundwater, ingested soil and vegetation, and, in the post-medieval and modern era, environmental levels can be locally elevated through industrial processes and agricultural practices (National Research Council, 2005: 154, 157–8; Weinstein and Davison, 2004: 71; WHO 2002: 20–3, 159). As herbivores, cattle are more susceptible than many other species to chronic fluoride toxicity (Franke, 1989; Craig et al., 2015: 84; Weinstein and Davison, 2004: 70) due to their digestive system and potential calcium deficiency brought on by milk production in cows (Franke, 1989). A poor diet may further increase susceptibility (Craig et al., 2015: 84). Osteofluorotic PNB growth first occurs bilaterally on the proximal medial metatarsals and may also involve other distal limb bones, ribs and mandible, with exostoses often, but not exclusively, developing at sites of fascial or tendinous insertions, and not commonly involving articular surfaces (National Research Council, 2005: 160; Craig et al., 2015: 85–86). Whilst the Groundwell individual's one surviving metatarsal did exhibit PNB, the deposits do not seem to favour locations of musculo-tendinous insertion on the metatarsal nor phalanges. In any event, osteofluorosis seems an unlikely diagnosis given that Britain lies outside the zone of high levels of naturally occurring fluoride (Weinstein and Davison, 2004: 8–9) and therefore endemic fluorosis, as observed in human populations (Ortner and Schutkowski, 2008 110–13).

Copper deficiency may lead to PNB production and focal thickenings in metaphyseal cartilage, which may give rise to marked expansion of the distal metapodials in cattle (Smart et al. 1980; Smart et al. 1981: 373; Craig et al., 2015: 81). Osteoporosis can also develop, due to copper's role in cross-linking collagen and elastin (Smart et al. 1981: 373; Craig et al., 2015: 66). These features differ from those seen in the Groundwell remains.

Panosteitis is the endosteal proliferation on new bone, centred in the regions of long bone nutrient foramina that in some cases may lead to periosteal bone proliferation, its aetiology is unknown (Roush, 2006, Craig et al., 2015: 106–107, Kieves, 2021: 369–376). Panosteitis is chiefly a disease of young dogs (Craig et al., 2015: 106), however, a single suspected case has been reported in a young camel (Levine et al., 2007) and a second in a 1.5-month-old calf (Sato et al., 2015). While the tendency for bone deposition in panosteitis to focus around nutrient foramina encourages comparison with the Groundwell phalanges, radiography and CT examination indicated no endosteal proliferation of bone in the recovered specimens (Fig. 4, 5, 6 and 7), opposing this diagnosis.

Peripheral gangrene may occur in cattle as a result of *Salmonella* infection (Mee, 1995), ergotism (Fraser and Dorling, 1983), or other causes. Bony involvement may occur, and lead to PNB formation in gangrenous parts. However, the inter- and intra-element patterning in PNB in the current case is not consistent with that expected in such instances (cf. Fraser and Dorling, 1983; Mee, 1995).

Unusually for faunal palaeopathology, we have all four limbs from

Fig. 5. Cattle metatarsal. Anterior aspect (top left) showing diffuse subperiosteal new bone on diaphysis, with detail of proximal diaphysis (bottom) photographed using a Keyence VHX7000 3-D digital microscope at x20 magnification (AHRC Award AH/V011758/1). Radiographs showing anterior-posterior (top, centre. x-ray P3321) and medio-lateral (top, right, x-ray P3323) views. © Historic England.

one animal, aiding differential diagnosis. Nevertheless, the sparseness of the remains means that firm diagnosis is difficult. While we cannot conclusively exclude the possibility of other conditions, the bilaterally symmetric distribution, and the similar morphology and location of lesions on the phalanges, are consistent with HO and allow us to advance this diagnosis over the other options discussed above. We did not find evidence of *M. tuberculosis* complex DNA, which has been identified in archaeological human (Mays and Taylor, 2002; Masson et al., 2013) and canine (Bathurst and Barta, 2004) HO cases, but this does not preclude HO as a diagnosis for the lesions.

The rather poorly remodelled nature of the lesions suggests that they represent an early stage of skeletal involvement. The focus of the deposits around foramina in the second phalanges is intriguing and we cannot find any parallels in the faunal palaeopathological literature. Bone formation around foramina may occur due to haemorrhage, for example in scurvy in humans (Brickley and Mays, 2019), but vitamin C deficiency does not induce this disease in cattle (Thurston et al., 1926; Craig et al., 2015: 83). In HO, while there is no suggestion of haemorrhagic lesions, increased blood flow in the extremities is a consistent and early feature (Martin et al., 1971; Craig et al., 2015: 93, Vengušt et al. 2018) and whether that would potentially cause bony alterations around foramina is not clear.

Finally, the lesions on phalanges 2A and 2D are evidenced by remnant PNB and discolouration demarking their former extent. It is likely that the deposits were detached through mechanical damage during excavation or subsequent archaeological processing, highlighting the fragile nature of some palaeopathological evidence and the need for care when handling archives.

6. Conclusions

HO is the most likely differential diagnoses, and if correct would be the first palaeopathological case reported in cattle, and one of very few diagnosed from zooarchaeological material. However, our diagnosis is tentative, restricted by both the incomplete skeletal representation of the specimen and the rarity of the disease in modern cattle.

Modern cases of HO in cattle are secondary to pulmonary disease (Ravary and Fecteau, 2000) including pneumonia (Merritt et al., 1971, Schelcher et al., 1989), carcinoma (Guyot et al., 2011; László, 1929), tracheobronchitis with a mummified foetus (Martin et al. 1971), or to gluteal and spleen abscesses (Hofmeyr, 1964). In other non-human taxa, it can be secondary to a variety of thoracic and abdominal conditions (for example, Watrous and Blumenfeld, 2002, 546–8). Apart from symptoms attributable to the primary condition, HO in cattle (as in other quadrupeds) is generally associated with lameness (Greenough et al., 1972: 299–300), and animals may be reluctant to rise to a standing position (e.g. Martin et al., 1971). The presence of the condition in ancient herds has implications for animal management in the past so its identification in early remains of domestic livestock is of broader interest. Remains of such animals normally end up fragmented and disarticulated in food waste residues, and the suggestion of HO in the present case has rested largely on the fact that zooarchaeological analyses allowed us to infer that the remains represented a bone group from a single individual, when that was not evident in the field. The case serves as a reminder of the importance of looking for skeletal patterning in seemingly disarticulated and comingled remains.

In the Groundwell Villa case, the element representation, together with butchery-mark evidence, suggests that they represent waste from leather production, whereby the feet and horncores were retained with the skin after primary butchery and discarded in demolition contexts at the villa at the start of the tanning process (see Albarella, 2003; Shaw, 1996: 107). Retaining the horncores with the skin may have allowed the tanner to establish the age of the animal (Serjeantson, 1989). The presence of skinning marks on several bones indicates that the skin had been removed before the bones were dumped. If suffering from initial stages of HO, the Groundwell animal may not have been in poor body condition compared to its contemporaries, but lameness and/or symptoms associated with the primary disease may have limited the animal's perceived economic value and led to its selection for slaughter. The presence of HO would have been inconsequential for the value of the hide, as it does not affect skin or hair (Martin et al., 1971).

Given the centrality to diagnosis of demonstrating bilaterally

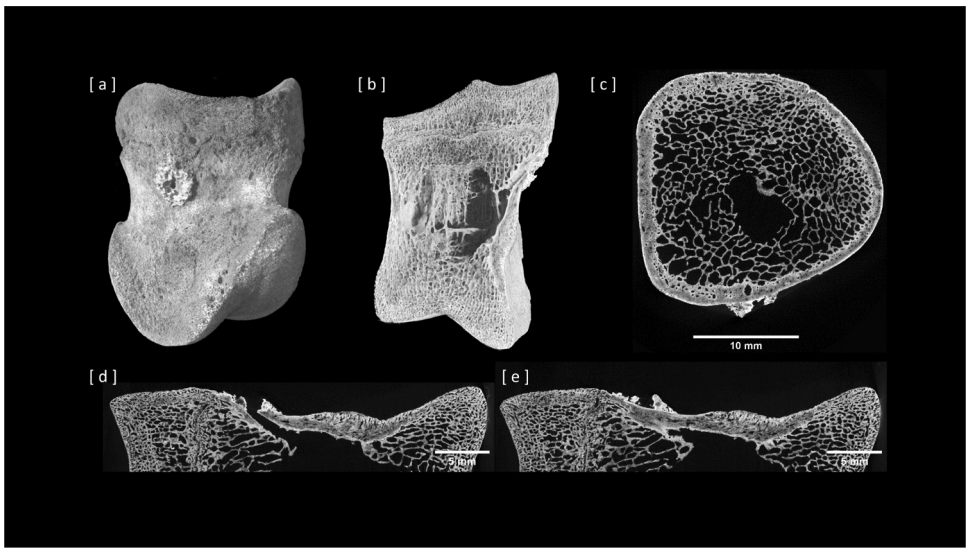

Fig. 6. µCT visualisation. 3D photorealistic rendering of phalanx 2C providing an overview of its structure and the subperiosteal new bone deposit focused on a foramen (a, top left); virtual crop of the 3D rendering revealing the vascular canal and inner trabecular architecture (b, top centre); 2D transverse (XY) slice captured at the defect level (defect seen at bottom of view) (c, top right); 2D longitudinal (YZ) slice across the canal (d, bottom left) and adjacent to it (e, bottom right), showing the surface development of deposited bone tissue around the vascular canal. Images b to e indicated no endosteal proliferation of bone (full dataset available at https://doi.org/10.5281/zenodo.8262662).

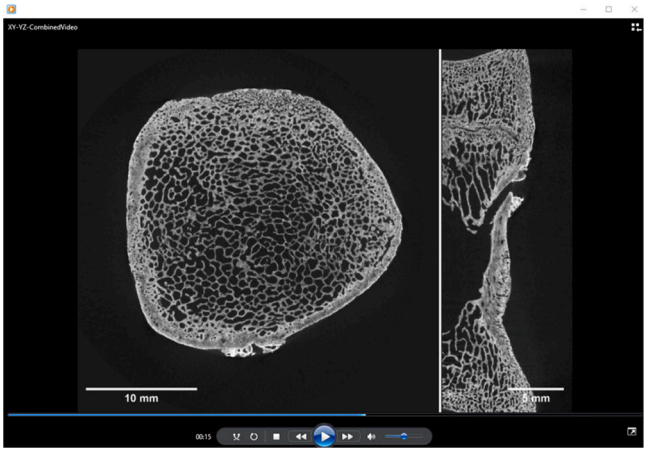

Fig. 7. Still image captured from Supplementary Information **Video 1**. Side-by-side single-slice roll of transverse (XY) and longitudinal (YZ) planes shown in Figs. 6c and 6d/6e respectively. The roll is focused around the defect (full dataset available at https://doi.org/10.5281/zenodo.8262662).

Fig. 8. Still image captured from Supplementary Information **Video 2**. 360-degree radiographic inspection of the phalanx. The radiographs were captured during the µCT acquisition process and serve as the basis for reconstructing the volumetric image.

symmetrical lesions in individual animals, HO is only likely to be reliably identified in articulated remains or, as in the present suggested case, bone groups that can reasonably be ascribed to single individuals on archaeological grounds.

Funding

This research did not receive any specific grant from funding agencies in the public, commercial, or not-for-profit sectors.

CRediT authorship contribution statement

Fay Worley: Writing – review & editing, Writing – original draft, Visualization, Resources, Methodology, Formal analysis, Data curation, Conceptualization. **Katsamenis Orestis:** Writing – review & editing, Writing – original draft, Visualization, Resources, Methodology, Formal analysis, Data curation. **G. Michael Taylor:** Writing – review & editing, Writing – original draft, Visualization, Resources, Methodology, Formal analysis, Data curation. **Simon Mays:** Writing – review & editing, Writing – original draft, Methodology, Formal analysis.

Acknowledgements

The authors would like to thank Peter Wilson (Rarey Archaeology; formerly of Historic England) for allowing us to present and publish this work in advance of the excavation's primary publication. We also acknowledge the µ-VIS X-ray Imaging Centre (www.muvis.org) at the University of Southampton, founding partner of the UK National Research Facility for lab-based X-ray computed tomography (EPSRC grant EP/T02593X/1), for the provision of the µCT imaging facilities, data processing and management infrastructure and Karla Graham for

providing details of the x-radiography equipment at Historic England. Finally, thank you to the two anonymous reviewers for their helpful comments.

Appendix A. Supporting information

Supplementary data associated with this article can be found in the online version at doi:10.1016/j.ijpp.2025.11.003.

References

Albarella, U., 2003. Tawyers, tanners, horn trade and the mystery of the missing goat. In: Murphy, P., Wiltshire, P.E.J. (Eds.), The Environmental Archaeology of Industry. Oxbow, Oxford, pp. 71–86.

Allan, G.S., 2007. Radiographic signs of joint disease in dogs and cats. In: Thrall, D.E. (Ed.), Textbook of Veterinary Diagnostic Radiology. Elsevier Saunders, St Louis.

Allen, M., 2017. Pastoral farming. In: Allen, M., Lodwick, L., Brindle, T., Fulford, M., Smith, A. (Eds.), The Rural Economy of Roman Britain. Britannia Monograph Series 30. London, Society for the Promotion of Roman Studies, pp. 142–177.

Armitage, P., 1982. A system for ageing and sexing the horncores of cattle from British post-medieval sites (with special reference to unimproved British longhorn cattle). In: Wilson, B., Grigson, C., Payne, S. (Eds.), Ageing and Sexing Animal Bones from Archaeological Sites, BAR British Serries, 109. British Archaeological Reports, Oxford, pp. 37–54.

Baker, J., Brothwell, D., 1980. Animal Diseases in Archaeology. Academic Press, London.

Bartosiewicz, L., 1993. The anatomical position and metric traits of phalanges in cattle (Bos taurus., 1758). Rev. De. Paléobiologie 2 (12), 325–334.

Bathurst, R.R., Barta, J.L., 2004. Molecular evidence of tuberculosis induced hypertrophic osteopathy in a 16th-century Iroquoian dog. J. Archaeol. Sci. 31, 917–925.

Becker, T.J., Perry, R.L., Watson, G.L., 1999. Regression of hypertrophic osteopathy in a cat after surgical excision of an adrenocortical carcinoma. J. Am. Anim. Hosp. Assoc. 35 (6), 499–505. https://doi.org/10.5326/15473317-35-6-499. PMID: 10580910.

Bom, H.A.S.C., Silva Filho, G.B., Fonseca, S.M.C., Lima, S.C., Rizzo, H., Almeida, V.M., Souza, F.A.L., Medonça, F.S., 2020. Hypertrophic osteoarthropathy in a sheep. Ciência Rural 50 (12). https://doi.org/10.1590/0103-8478cr20191038.

Brickley, M.B., Mays, S., 2019. Metabolic disease. In: Buikstra, J.E. (Ed.), Ortner's Identification of Pathological Conditions in Human Skeletal Remains, 3rd. Elsevier, London, pp. 531–566.

Brodey, R.S., 1971. Hypertrophic osteoarthropathy in the dog: a clinicopathologic survey of 60 cases'. J. Am. Vet. Med. Assoc. 159 (10), 1242–1256.

Cetinkaya, M.A., Yardimci, R., Yardimci, C., 2011. Hypertropic osteopathy in a dog associated with intra-thoracic lesions: a case report and a review. Vet. Med. 56 (12), 595–601. https://doi.org/10.17221/4437-VETMED.

Craig, L.E., Dittmer, K.E., Thompson, K.G., 2015. Bones and joints. In: Grant Maxie, M. (Ed.), Jubb, Kennedy and Palmer's Pathology of Domestic Animals, 5th. Elsevier, London, pp. 17–163.

Dottrens, E., 1946. Etude préliminaire: les phalanges osseuses des Bos taurus domesticus. Rev. Suisse Zool. 53, 739–744.

Drexler, L., 1957. Ein pathologisher humerus eines Höhlenbären. Ann. Des. Nat. Mus. Wien. 61, 96–101.

Enright, K., Tobin, E., Katz, L.M., 2011. A review of 14 cases of hypertrophic osteopathy (Marie's disease) in horses in the Republic of Ireland. Equine Vet. Educ. 23, 224–230. https://doi.org/10.1111/j.2042-3292.2010.00139.x.

Franke, J., 1989. Differences in skeletal response to fluoride in humans and animals: an overview. Fluoride 22 (1), 10–19.

Fraser, D.M., Dorling, P.R., 1983. Suspected ergotism in two heifers. Aust. Vet. J. 60, 303–305. https://doi.org/10.1111/j.1751-0813.1983.tb02814.x.

Gall, E.A., Bennett, G.A., Bauer, W., 1951. Generalised hypertrophic osteoarthropathy. Am. J. Pathol. 27, 349–385.

Greenough, P.R., MacCallum, F.J., Weaver, D.A., 1972. Lameness in Cattle. Oliver and Boyd, Edinburgh.

Guyot, H., Sandersen, C., Rollin, F., 2011. A case of hypertrophic osteoarthropathy in a Belgian blue cow. Can. Vet. J. 52 (12), 1308–1311.

Heacock, E., Bates, A., Wulster, K., Manzi, T., Luethy, D., Abrahamb, M., 2020. Hypertrophic osteopathy in a pregnant doe with bronchopneumonia. Clin. Theriogenol. 12 (4). https://doi.org/10.58292/ct.v12.9451.

Helmer, D., 1987 Fiches descriptives pour les relevés d'ensembles osseux animaux in Desse, J. and Desse-Berset, N. Fiches d'ostéologie animale pour l'archéologie, Série B: mammifères, n° 1. Juan-les-Pins: Centre de recherches archéologiques du CNRS / APDCA, Fig. 5.

Hofmeyr, C.F.B., 1964. Hypertrophische Osteo-Arthropathie (Acropachia, Marie's Disease) bei einem Bullen. *Berliner und Münchener Tierärztliche*. Wochenschrift 77, 319–321.

Huang, Chiung-Hui, Jeng, Chain-Ren, Lin, Chung-Tien, Yeh, Lih-Seng, 2010. Feline hypertrophic osteopathy: a collection of seven cases in Taiwan. J. Am. Anim. Hosp. Assoc. 46, 346–352. https://doi.org/10.5326/0460346.

Johnson, K.A., Watson, A.D.J., 2000. Skeletal diseases. In: Ettinger, S (Ed.), Textbook of Veterinary Internal Medicine, 5th edition. W. B. Saunders, Philadelphia, PA, USA, pp. 1903–1904.

Kieves, N.R., 2021. Juvenile disease processes affecting the forelimb in canines. Vet. Clin. North Am. Small Anim. Pract. 51 (2), 365–382. https://doi.org/10.1016/j.cvsm.2020.12.004. PMID: 33558013.

László, P., 1929. Akropachia szarvasmarhában. Állatorvorsi Lapok 52 (16), 191–194.

Lawler, D.F., Reetzs, J.A., Sackman, J.E., Evans, R.H., Widga, C., 2015. Suspected hypertrophic osteopathy in an ancient canid; differential diagnosis of possible etiologies. Int. J. Palaeopathol. 9, 52–58. https://doi.org/10.1016/j.ijpp.2015.02.001.

Levine, D.G., Smith, J.J., Richardson, D.W., Brown, V., Beech, J., Habecker, P., Adam, E., 2007. Suspected panosteitis in a camel. J. Am. Vet. Med. Assoc. 231 (3), 437–441. https://doi.org/10.2460/javma.231.3.437. PMID: 17669048.

Lewis, N.L., Leadon, D., Sharp, W.B., Gibbons, P.T., Antignani, M., 2011. Resolution of hypertrophic osteopathy in a 2-year-old filly. Equine Vet. Educ. 23, 217-223.

Loyer, J., Murphy, E., Ruppe, M., Moiseyev, V., Khartanovich, V., Zammit, J., Rottier, S., Potrakhov, N., Bessonov, V., Obodovskiy, A., 2019. Co-morbidity with hypertrophic osteoarthropathy: a possible Iron Age Sarmatian case from the Volga steppe of Russia. Int. J. Palaeopathol. 24, 66–78. https://doi.org/10.1016/j.ijpp.2018.09.007.

Luff, R., Brothwell, D., 1993. Health and welfare. In: Luff, R. (Ed.), Animal Bones from Excavations in Colchester, 1971-85. Colchester Archaeological Report 12. Colchester Archaeological Trust, Colchester, pp. 101–126.

Marinkovich, M., Wisner, E.R., Brenner, D.J., 2019. Distal limb swelling and periosteal productive reaction in periparturient Sichuan takin (*Budorcas taxicolor tibetana*): five cases of presumptive hypertrophic osteopathy. J. Zoo. Wildl. Med. 50 (2), 437–446. https://doi.org/10.1638/2018-0174.

Martin, S.W., Pennock, P.W., Pass, D., 1971. Hypertrophic pulmonary osteoarthropathy in a cow. Can. Vet. J. 12 (6), 129–131.

Masson, M., Molnár, E., Donoghue, H.D., Besra, G.S., Minnikin, D.E., Wu, H.H.T., Lee, O. Y.-C., Bull, I.D., Pálfi, G., 2013. Osteological and Biomolecular evidence of a 7000-year-old case of hypertrophic pulmonary osteopathy secondary to tuberculosis from Neolithic Hungary. PLOS One 8 (10), e78252. https://doi.org/10.1371/journal.pone.0078252.

Mays, S., Taylor, G.M., 2002. Osteological and biomolecular study of two possible cases of hypotrophic osteoarthropathy from mediaeval England. J. Archaeol. Sci. 29, 1267–1276. https://doi.org/10.1006/JASC.2001.0769.

Meadows, J., Bayliss, A., Bronk Ramsey, C., Cook, G., Hamilton, D., Marshall, P., Morley, G., Wilson, P., 2012. Groundwell Ridge, Swindon, Wiltshire: Radiocarbon Dating and Chronological Modelling. Research Report Series 24-2012. English Heritage, London.

Mee, J.F., 1995. Terminal gangrene and ostitis in calves attributed to *Salmonella dublin* infection. Irish Veterinary Journal 48, 22–28.

Merritt, A.M., Dodd, D.C., Reid, C.F., Boucher, W.B., 1971. Hypertrophic pulmonary osteopathy in a steer. J. Am. Vet. Med. Assoc. 159, 443–448.

Morley, G., Wilson, P., 2025. The Groundwell Ridge Villa Baths Building. Wiltshire Archaeology & Natural History Magazine 118, 135–158.

Morley, G. and Wilson, P. 2024 Groundwell Roman Villa. Final report on the 2003-2005 Excavations at Groundwell Ridge, Swindon. Historic England Research Report Series 60/2024.

National Research Council, 2005. Mineral Tolerance of Animals, 2nd. National Academy of Sciences, Washington, D.C.

Ortner, D.J., Schutkowski, H., 2008. Ecology, culture and disease in past populations. In: Schutkowski, H. (Ed.), Between Biology and Culture. Cambridge University Press, Cambridge, pp. 105–128.

Peters, J., 1988. Osteomorphological features of the appendicular skeleton of Africa buffalo, *Syncerus caffer* (Sparrman, 1799) and of domestic cattle, *Bos primigenius* f. Taurus Bojanus, 1827. Z. F. üR. Säugetierkunde 53, 108–123.

Ravary, B., Fecteau, G., 2000. Two cases of bovine hypertrophic osteopathy (Marie-Bamberger's disease). Point Vet. 31, 71–77.

Resnick, D., Niwayama, G., 1981. Diagnosis of Bone and Joint Disorders, 1st edition. WB Saunders, Philadelphia.

Resnick, D., Niwayama, G., 1995. Diagnosis of Bone and Joint Disorders, 3rd. WB Saunders, Philadelphia.

Roush, J.K., 2006. Chapter 117 - Miscellaneous diseases of bone, in Birchard, S.J. and Sherding, R.G. (eds), Saunders Manual of Small Animal Practice. 3rd edition, W.B. Saunders: pp. 1186-1193, https://doi.org/10.1016/B0-72-160422-6/50119-4.

Sato, R., Ito, T., Suganama, T., Une, Y., Kudo, T., Kayanuma, H., Kanai, E., Suzuki, T., Ochiai, H., Enomoto, N., Itoh, S., Onda, K., Wada, Y., 2015. Suspected panosteitis in a crossbred calf. Can. Vet. J. 56, 463–465.

Schelcher, F., Autefage, A., Delverdier, M., Espinasse, J., Bezille, P., Jouglar, J.-Y., 1989. Ostéopathie hypertrophiante: observation chez un veau. Rev. MéD. V. ét 140, 567–571.

Serjeantson, D., 1989. Animal remains and the tanning trade. In: Serjeantson, D., Waldron, T. (Eds.), Diet and Crafts in Town. The Evidence of Animal Remains from the Roman to the Post-Medieval Period. BAR British Series 199. British Archaeological Reports, Oxford, pp. 129–146.

Shaw, M., 1996. The excavation of a late 15th- to 17th –century tanning complex at The Green, Northampton. PostMediev. Archaeol. 30, 63–127.

Silver, I.A., 1969. The ageing of domestic animals. In: Brothwell, D., Higgs, E. (Eds.), Science in Archaeology. Thames and Hudson, London, pp. 283–302.
Smart, M.E., Gudmundson, J., Christensen, D.A., 1981. Trace mineral deficiencies in cattle: a review. Can. Vet. J. 22, 372–376.
Smart, M.E., Gudmundson, J., Brockman, R.P., Cymbaluk, N., Doige, C., 1980. Copper deficiency in calves in northcentral Manitoba. Can. Vet. J. 21, 349–352.
Thurston, L.M., Eckles, C.H., Palmer, L.S., 1926. The role of the antiscorbutic vitamin in the nutrition of calves. J. Dairy Sci. 9, 37–49.
Vengušt, G., Žele, D., Švara, T., Dolenšek, T., 2018. Hypertrophic osteopathy associated with mycotic pneumonia in a roe deer (*Capreolus capreolus*). J. Wildl. Dis. 54 (3), 631–634. https://doi.org/10.7589/2017-07-171.
Watrous, B.J. and, Blumenfeld, B., 2002. Congenital megaesophagus with hypertrophic osteopathy in a 6-year-old dog. Vet. Radio. Ultrasound 43 (6), 5459. https://doi.org/10.1111/j.1740-8261.2002.tb01046.x.
Weinstein, L.H., Davison, A.W., 2004. Fluorides in the Environment. CABI Publishing, Wallingford.
Weston, D.A., 2008. Investigating the specificity of periosteal reactions in pathology museum specimens. Am. J. Phys. Anthropol. 137, 48–59. https://doi.org/10.1002/ajpa.20839.
Weston, D.A., 2009. Palaeohistological analysis of pathology museum specimens: can periosteal reaction microstructure explain lesion etiology? Am. J. Phys. Anthropol. 140, 186–193. https://doi.org/10.1002/ajpa.21081.
Withers, S.S., Johnson, E.G., Culp, W.T.N., Rodriguez, C.O., Skorupski, K.A., Rebhun, R. B., 2013. Paraneoplastic hypertrophic osteopathy in 30 dogs. Vet. Comp. Oncol. 13 (3), 157–165. https://doi.org/10.1111/vco.12026.
World Health Organisation, 2002. Environmental health criteria 227: fluorides. World Health Organisation, Geneva.